Mixture of Spherical Distributions for Single-View Relighting

Kenji Hara, *Member*, *IEEE*, Ko Nishino, *Member*, *IEEE*, and Katsushi Ikeuchi, *Fellow*, *IEEE*

Abstract—We present a method for simultaneously estimating the illumination of a scene and the reflectance property of an object from single view images—a single image or a small number of images taken from the same viewpoint. We assume that the illumination consists of multiple point light sources, and the shape of the object is known. First, we represent the illumination on the surface of a unit sphere as a finite mixture of von Mises-Fisher distributions based on a novel spherical specular reflection model that well approximates the Torrance-Sparrow reflection model. Next, we estimate the parameters of this mixture model including the number of its component distributions and the standard deviation of them, which correspond to the number of light sources and the surface roughness, respectively. Finally, using these results as the initial estimates, we iteratively refine the estimates based on the original Torrance-Sparrow reflection model. The final estimates can be used to relight single-view images such as altering the intensities and directions of the individual light sources. The proposed method provides a unified framework based on directional statistics for simultaneously estimating the intensities and directions of an unknown number of light sources, as well as the specular reflection parameter of the object in the scene.

Index Terms—Inverse rendering, von Mises-Fisher distribution, finite mixture distribution, EM algorithm.

1 Introduction

Recovering photometric information of real-world objects and scenes from their images and 3D geometric models and synthesizing images of the same objects and scenes under arbitrary novel illumination conditions have been studied as inverse rendering and relighting mainly in the computer vision and graphics communities. The more information about the object and the scene in the image we estimate, such as the directions and colors of the illumination and surface properties of objects, the wider variety of virtual editing of the original image we can accomplish.

A variety of inverse rendering methods have been proposed to estimate illumination from single-view images, for example, from a single image or a sequence of images captured from the same point. These methods range from those limited to simple illumination consisting of only a single light source [23] to those that handle more complex illumination with multiple light sources [38], [42], [10], [16], [12], [26], [41], [34], [35], [14], [22]. These methods, however, assume the surface reflectance to be known or to be Lambertian.

Instead of only estimating the illumination or the reflectance property of objects in a scene [8], [5], [2], several approaches that recover both of them for single-view relighting have been proposed [11], [31], [25], [17], [9]. Such joint estimation methods can be classified into two categories: spatial domain methods [11], [31], [17], [9] and frequency domain methods [25]. Although decoupling of illumination and reflectance can be better described in the frequency domain, relighting such as directly manipulating the intensities and directions of the recovered light sources can be achieved more naturally in the spatial domain. In our framework, we adopt a spatial domain-based joint estimation method using mixtures of spherical distributions as the core representation of the illumination and surface properties.

Much of the spatial domain methods for illumination estimation assume that 1) all the light sources are infinitely distant (that is, directional light sources), 2) the geometry of the target object is known, and 3) the number of light sources is known. In this paper, we propose a novel method for simultaneously estimating both the illumination of a scene and the reflectance property of a real object in the scene, given single-view images taken under multiple point light sources and a geometric model of the object. Unlike previous methods, our method can recover not only the direction and intensity of multiple light sources but also the number of light sources and the specular reflectance property of the object. This eliminates one of the above general assumptions making the method more practical. We accomplish this by deriving a novel spherical specular reflection model based on the Torrance-Sparrow reflection model [32] to model the illumination and the surface property as a mixture of spherical distributions. It is exactly this combination of 1) reformulation of specular reflection and illumination as mixtures of spherical distributions and 2) the careful adoption of well established machine learning algorithm for solving the mixtures that enables automatic estimation of the illumination distribution, the reflectance parameters, and the number of light sources. The results demonstrate, for the first time, the advantage of using a rigorous directional statistics approach for appearance modeling.

First, using the specular reflection component separated from the input image, we represent the illumination condition as a finite mixture of von Mises-Fisher distributions [37], [7] on the unit sphere based on a spherical representation of specular

- *K. Hara is with the Department of Visual Communication Design, Faculty of Design, Kyushu University, 4-9-1, Shiobaru, Minami-ku, Fukuoka, 815-8540, Japan. E-mail: hara@design.kyushu-u.ac.jp.*
- *K. Nishino is with the Department of Computer Science, College of Engineering, Drexel University, 3141 Chestnut Street, Philadelphia, PA 19104. E-mail: kon@drexel.edu.*
- *K. Ikeuchi is with the Institute of Industrial Science, The University of Tokyo, 4-6-1 Komaba, Meguro-ku, Tokyo 153-8505, Japan. E-mail: ki@cvl.iis.u-tokyo.ac.jp.*

Manuscript received 2 Oct. 2006; revised 6 Apr. 2007; accepted 16 Apr. 2007; published online 30 Apr. 2007.
Recommended for acceptance by R. Basri.
For information on obtaining reprints of this article, please send e-mail to: tpami@computer.org, and reference IEEECS Log Number TPAMI-0698-1006.
Digital Object Identifier no. 10.1109/TPAMI.2007.1164.

reflection. Then, by using the Expectation-Maximization (EM) algorithm, we estimate the mixture parameters that correspond to both the illumination distribution and the reflectance parameter. Finally, using the results as initial estimates, we solve an optimization problem using the original specular reflection model in Cartesian coordinates. The results allow us to render the object under novel lighting conditions.

The remainder of the paper is organized as follows: In Section 2, we explain the von Mises-Fisher distribution defined on the surface of a sphere. Using this distribution model, we derive a novel spherical specular reflection model based on the Torrance-Sparrow reflection model. Next, in Section 3, we describe how to represent the specular reflection as a mixture of spherical distributions and how to formulate the illumination estimation problem as a mixture estimation problem. Then, we show how we can estimate both the parameters of each distribution and the number of components of the mixture. In Section 4, we show experimental results on synthetic and real images. Finally, we conclude in Section 5.

2 A Reflection Model Based on Spherical Distribution

Surface reflection of general inhomogeneous surfaces can be modeled as a linear combination of diffuse and specular reflection components [27], [13]. To model the specular component, we use the Torrance-Sparrow reflection model [32], which is widely known to approximate the specular reflection well [19]. The Torrance-Sparrow reflection model assumes that the object surface is made of mirrorlike microscopic facets (*microfacets*) distributed in V-shaped grooves as

$$\mathbf{I}_S = \int_\Omega \frac{\mathbf{K}_S F G}{\cos\theta_r} L_i(\theta_i, \phi_i) \exp\left[-\frac{\alpha^2}{2\sigma^2}\right] d\omega_i, \tag{1}$$

where $\mathbf{I}_S$ denotes a three-band color vector of the specular reflection radiance, $\mathbf{K}_S$ is the color vector of the specular reflection (which includes the normalization factor of the exponential function, the reflectivity of the surface, and the scaling factor between scene radiance and a pixel value), F is the Fresnel reflectance coefficient, G is the geometrical attenuation factor, θ_r is the angle between the viewing direction and the surface normal, θ_i and ϕ_i are the altitude and azimuth coordinates, respectively, $L_i(\theta_i, \phi_i)$ is the illumination radiance per unit solid angle coming from the direction (θ_i, ϕ_i), $d\omega_i$ is the infinitesimal solid angle ($d\omega_i = \sin\theta_i d\theta_i d\phi_i$), α is the angle between the surface normal and the bisector of the viewing direction and the light source direction, and σ is the surface roughness.

From (1), we can clearly see that the Torrance-Sparrow reflection model approximates the distribution of the orientations of microfacets with a Gaussian distribution with mean zero and standard deviation σ. In this section, we derive a specular reflection model based on a spherical distribution (or a directional distribution) instead of the Gaussian distribution, and we show that this reflection model can well approximate the Torrance-Sparrow reflection model.

2.1 The Von Mises-Fisher Distribution

To analyze statistically directional data, the von Mises-Fisher (hereafter referred to as vMF) distribution [37], [7] has been widely used because of its analogy to the Gaussian distribution. A direction can be expressed by a point on a sphere of unit radius. A 3D unit random vector (that is, $\mathbf{x} = (x_1, x_2, x_3)^T$ satisfying $\|\mathbf{x}\| = 1$) is said to obey 3-variate vMF distribution if its probability density function is given by

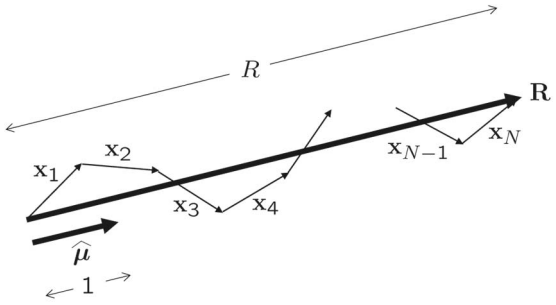

Fig. 1. Estimate of the mean direction.

$$f(\mathbf{x}|\,\boldsymbol{\mu}, \kappa) = \frac{\kappa}{4\pi\,\sinh\kappa} \exp\left[\kappa\,\mathbf{x}^T\boldsymbol{\mu}\right], \tag{2}$$

where $\boldsymbol{\mu}$ ($\|\boldsymbol{\mu}\| = 1$) is the mean direction, and $\kappa \geq 0$ is the concentration parameter. The concentration parameter κ characterizes how strongly the unit vectors drawn by $f(\mathbf{x}|\,\boldsymbol{\mu}, \kappa)$ are concentrated around the mean direction $\boldsymbol{\mu}$. Let $\chi = \{\mathbf{x}_1, \ldots, \mathbf{x}_N\}$ be a data set of N random unit vectors (a set of directions) following a vMF distribution model. Let $\mathbf{R}$ be the vector sum (resultant vector) of these vectors: $\mathbf{R} = \sum_{i=1}^N \mathbf{x}_i$, as shown in Fig. 1. Then, the standard estimate $\hat{\boldsymbol{\mu}}$ of the mean direction can be computed by simply normalizing the resultant vector $\mathbf{R}$. The standard estimate $\hat{\kappa}$ of the concentration parameter is, when the true mean direction is unknown, given by that in [7], [15]

$$\hat{\kappa} = \frac{N-1}{N-R}, \tag{3}$$

where $R = \|\mathbf{R}\| = \sum_{i=1}^N \mathbf{x}_i^T \hat{\boldsymbol{\mu}}$ is the resultant vector length, as shown in Fig. 1.[1]

The density function (2) can be rewritten in terms of a spherical polar coordinate system as follows:

$$f'(\theta, \phi\,|\,\boldsymbol{\mu}, \kappa) = \frac{\kappa}{4\pi\,\sinh\kappa} \exp[\kappa\cos\theta], \tag{4}$$

where $\theta \in [0, \pi]$ and $\phi \in [0, 2\pi]$ are the polar and azimuth angles from the mean direction, respectively.

2.2 The Spherical Torrance-Sparrow Model

Let $\mathbf{S}$ be the directional vector mirror symmetric to the surface normal $\mathbf{N}$ with respect to the normal $\mathbf{H}$ of the microfacet (Fig. 2a). We assume that $\mathbf{S}$ obeys a vMF distribution with mean direction $\mathbf{N}$ (Fig. 2b). More specifically, the probability of finding a direction $\mathbf{S}$ within a unit angular area centered at an angle, (θ, ϕ), from the surface normal direction $\mathbf{N}$ is given by (4). Now, $\theta \in [0, \pi]$ is clearly equal to twice the angle, α (α in (1)), between $\mathbf{N}$ and $\mathbf{H}$. Hence, this probability is proportional to $\exp[-2\kappa\sin^2\alpha]$, since $\exp[\kappa\cos\theta] = \exp[\kappa\cos 2\alpha] = \exp[\kappa]\exp[-2\kappa\sin^2\alpha]$. Similar to the derivation of the Torrance-Sparrow model, we replace the exponential function on the right side of (1) with $\exp[-2\kappa\sin^2\alpha]$ as follows:

1. The maximum likelihood (ML) estimates of $\boldsymbol{\mu}$ and κ are given by the above $\hat{\boldsymbol{\mu}}$ and $N/(N-R)$, respectively.

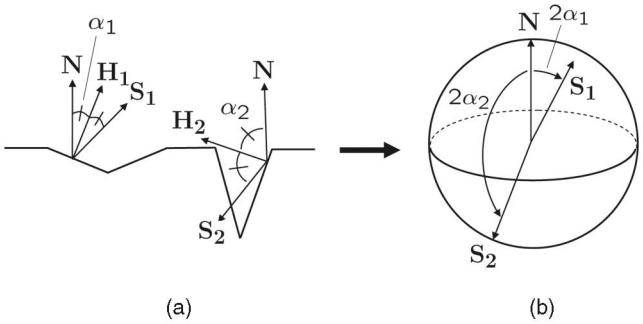

Fig. 2. Modeling the orientation of microfacet as a vMF distribution. We consider a mirror direction $\mathbf{S}$ of a microfacet opposite the surface normal direction $\mathbf{N}$ with respect to the microfacet normal $\mathbf{H}$. Supposing $\mathbf{N}$ is the north pole of a unit sphere, we can think of $\mathbf{S}$ as a point on the sphere, since the angle 2α between $\mathbf{S}$ and $\mathbf{N}$, namely, the polar angle, ranges from 0 to π. We assume that $\mathbf{S}$ has a vMF distribution with the mean direction equal to $\mathbf{N}$.

$$\int_{\Omega} \frac{\mathbf{K}_S FG}{\cos\theta_r} L_i(\theta_i, \phi_i) \exp\Big[-2\kappa \sin^2\alpha\Big] d\omega_i. \tag{5}$$

The concentration parameter κ here corresponds to the "smoothness" of the object surface. Also, we assume the following relation between the surface smoothness κ and surface roughness σ in such a manner that (5) is equivalent to (1) for small values of α (hence, $\sin\alpha \approx \alpha$):

$$\kappa = \frac{1}{4\sigma^2}. \tag{6}$$

On the other hand, it is well known that the Torrance-Sparrow reflection model can be simplified by redefining F and G as constant values, under the condition that the angle between the viewing and illumination directions is smaller than 60 degrees [29]. Thus, we also simplify (5) as

$$\mathbf{I}_S = \int_{\Omega} \frac{\mathbf{K}_S}{\cos\theta_r} L_i(\theta i, \phi_i) \exp\Big[-2\kappa \sin^2\alpha\Big] d\omega_i, \tag{7}$$

where $\mathbf{K}_S$ is redefined as $\mathbf{K}_S FG$. We call this specular reflection model the *spherical Torrance-Sparrow reflection model*.

Fig. 3 shows the approximation quality of the specular reflection radiance by the spherical Torrance-Sparrow model and the original Torrance-Sparrow model. From Fig. 3, we can see that these two simulation curves agree well when σ is within [0, 0.2] (it is known that σ generally takes between 0.001 and 0.2) and α is within [0, 60 degrees] (necessary condition for Torrance-Sparrow model simplification). This implies that the spherical Torrance-Sparrow model can be regarded as a good approximation to the Torrance-Sparrow model and, hence, also to the true specular reflection.

3 Multiple Light Sources and Reflectance Estimation

In this section, we formulate the illumination distribution as a mixture of vMF distributions on the unit sphere based on the spherical Torrance-Sparrow reflection model and then estimate the illumination and specular reflectance parameters as the mixture model parameters using the EM algorithm for this mixture model. The resulting estimates are then refined using a local optimization scheme based on the original Torrance-Sparrow reflection model.

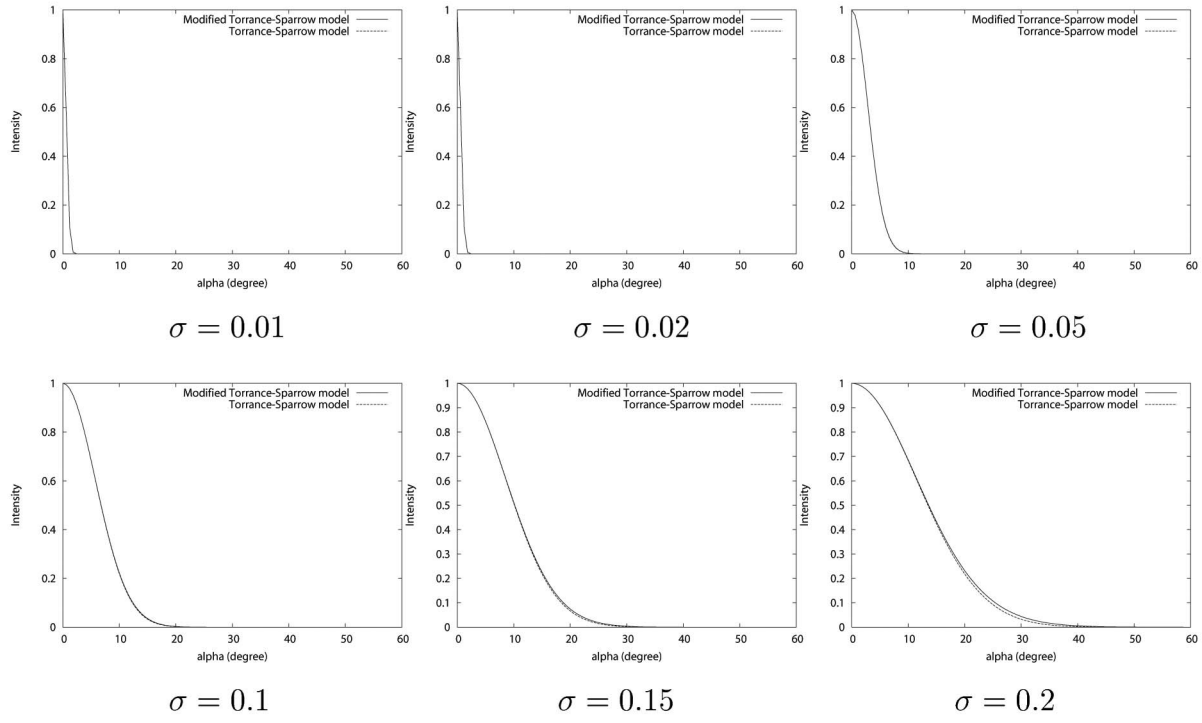

Fig. 3. Approximation of the specular reflection radiance, for a fixed σ, with respect to variations of α, by the spherical Torrance-Sparrow model (solid line), as well as the original Torrance-Sparrow model (dotted line). The curves agree well for all these cases showing that the spherical Torrance-Sparrow model approximates the original Torrance-Sparrow model extremely well.

3.1 A Mixture Representation of Illumination Condition

We assume that the scene is illuminated by a finite number of distant point light sources (that is, directional lights) that all have the same color. Also, the specular reflectance property of the object surface is assumed to be homogeneous. Then, (7) can be discretely approximated using the nodes of a geodesic dome [26], [21] as

$$\mathbf{I}_S \approx I_S \mathbf{L}, \tag{8}$$

$$I_S = \frac{2\pi}{N_L}\frac{K_S}{\cos\theta_r}\sum_{l=1}^{M_L} L_l \exp\Big[-2\kappa\sin^2\alpha_l\Big], \tag{9}$$

where $\mathbf{L}$ is the normalized color vector with the assumption that all the light sources have the same color, N_L is the number of the nodes of a geodesic dome in the northern hemisphere, M_L is the number of the point light source, L_l $(l = 1, \ldots, M_L)$ is the radiance of the lth light source, and α_l is the angle between the surface normal and the bisector of the viewing direction and the lth light source direction.

Now, suppose that light rays emanate in all directions from the viewpoint, some of the light rays pass through the image plane toward the object and strike the object surface. Then, we map the value of $\widetilde{I}_S = I_S\cos\theta_r = \sqrt{I_{S,R}^2 + I_{S,G}^2 + I_{S,B}^2}\cos\theta_r$ of each pixel to the mirror reflection direction at the corresponding surface point. We call the resulting scalar field on the unit sphere the *illumination sphere* [21].

The angle between this mirror reflection direction and the lth light source direction is given by $\psi_l = \arccos\big(\cos(2\alpha_l) + 2\sin^2\alpha_l\sin^2\theta_r\sin^2\phi_l\big)$, where ϕ_l is the azimuth angle of the bisector of the viewing direction and the lth light source direction from the surface normal. Since the specular reflection can only be observed when α_l has very small values, we ignore the second term and approximate ψ_l as $\psi_l \approx \arccos(\cos(2\alpha_l)) = 2\alpha_l$. Hence, the scalar value, $\widetilde{I}_S(\mathbf{x}\,|\,\Theta)$, of a location, $\mathbf{x}$, on the illumination sphere is represented as

$$\begin{aligned}\widetilde{I}_S(\mathbf{x}\,|\,\Theta) &= \frac{2\pi K_S}{N_L}\sum_{l=1}^{M_L} L_l \exp\Big[-2\kappa\sin^2\Big(\frac{1}{2}\arccos(\mathbf{x}^T\boldsymbol{\mu}_l)\Big)\Big] \\ &= \frac{2\pi K_S\,\exp[-\kappa]}{N_L}\sum_{l=1}^{M_L} L_l \exp\Big[\kappa\cos\Big(\arccos(\mathbf{x}^T\boldsymbol{\mu}_l)\Big)\Big] \\ &= \frac{2\pi K_S\,\exp[-\kappa]}{N_L}\sum_{l=1}^{M_L} L_l \exp\Big[\kappa\,\mathbf{x}^T\boldsymbol{\mu}_l\Big],\end{aligned} \tag{10}$$

where $\boldsymbol{\mu}_l$ is the direction of the lth light source, and $\Theta = \{L_1, \ldots, L_{M_L}, \boldsymbol{\mu}_1, \ldots, \boldsymbol{\mu}_{M_L}, \kappa\}$ is the set of the illumination and specular reflection parameters.

From (10) and (2), we can clearly see that the illumination sphere is equivalent to a mixture of vMF distributions

$$\widetilde{I}_S(\mathbf{x}\,|\,\Theta) = \sum_{l=1}^{M_L} L_l f(\mathbf{x}\,|\,\boldsymbol{\mu}_l, \kappa), \tag{11}$$

where L_l is redefined as the relative radiance of the lth light source so that $\sum_{l=1}^{M_L} L_l = 1$, $f(\cdot\,|\,\boldsymbol{\mu}_l, \kappa)$ is a vMF probability density function, and $\widetilde{I}_S(\mathbf{x}\,|\,\Theta)$ is also redefined as the relative irradiance on the illumination sphere normalized to unit probability

$$\int_0^{2\pi}\int_0^{\pi} \widetilde{I}_S(\mathbf{x}\,|\,\Theta)\sin\theta\,d\theta d\phi \approx \sum_{i=0}^{N'_L}\frac{4\pi}{N'_L}\widetilde{I}_S(\mathbf{x}_i\,|\,\Theta) = 1, \tag{12}$$

where $\mathbf{x}_i$ stands for the location of the node of a geodesic dome approximating a unit sphere, and N'_L is the number of the nodes of the geodesic dome. Also, 4π means that the entire sphere has a solid angle of 4π steradians.

As a result, the mixture weight, the number of components, the mean direction and concentration parameter of each component distribution correspond to L_l (the relative radiance of the lth light source), M_L (the number of the light source), $\boldsymbol{\mu}_l$ (the direction of the lth light source), and κ (the surface smoothness), respectively. Therefore, the problem of estimating illumination and specular reflection parameters can be formulated as a vMF mixture estimation problem with respect to $\Theta = \{L_1, \ldots, L_{M_L}, \boldsymbol{\mu}_1, \ldots, \boldsymbol{\mu}_{M_L}, \kappa\}$. Note that, unlike usual mixture estimation, the concentration parameter (or surface smoothness) κ is common to all the component distributions. This is because if κ is independently defined for each component distribution, each surface point has different reflectance properties for each light source, which physically does not make sense. Also note, under the assumption of the original Torrance-Sparrow model, the scalar field on the sphere is expressed as a linear combination of two dimensional Gaussian distributions for data in $\mathbf{R}^2$ so that the illumination estimation problem cannot be treated as a mixture estimation problem.

3.2 EM Algorithm for Illumination Sphere

We regard the problem of simultaneously estimating the multiple point light sources and the specular reflectance as a problem of estimating a mixture of vMF distributions, as described above. For estimating the parameters of a Gaussian mixture, the EM algorithm is widely used for its numerical stability and simplicity [4].

Recently, Banerjee et al. [1] proposed two variants (called the *hard-assignment scheme* and the *soft-assignment scheme*) of the EM algorithm for estimating the parameters of a mixture of vMF distributions. In this paper, we adopt Banerjee et al.'s EM algorithm for our parameter estimation problem. Note that their EM algorithm cannot be directly applied to our case, since our vMF mixture model, unlike the normal vMF mixture, includes the concentration parameter (κ), which is common to all the component distributions, as mentioned before. In order to deal with this problem, we introduce the hard-assignment scheme in the Expectation (E) step and an updating rule based on the estimate of the concentration parameter ((3)) in the Maximization (M) step. Also, for the parameters except κ, we use their soft-assignment scheme.

Now, let $\mathcal{X} = \{\mathbf{x}_1, \ldots, \mathbf{x}_N\}$ $(\|\mathbf{x}_i\| = 1, \forall i)$ be a set of samples drawn from the illumination sphere normalized as (12). Then, our EM algorithm randomly chooses M_L points (unit vectors) as the initial cluster means $\boldsymbol{\mu}_l$ $(l = 1, \ldots, M_L)$ and then iterates the following steps until convergence.

1. **E Step**. Update the distributions of the hidden variables for $i = 1, \ldots, N$ and $l = 1, \ldots, M_L$ as

$$p(l\,|\,\mathbf{x}_i, \Theta) \leftarrow \frac{L_l\, f(\mathbf{x}_i|\boldsymbol{\mu}_l, \kappa)}{\sum_{h=1}^{M_L} L_h\, f(\mathbf{x}_i|\boldsymbol{\mu}_h, \kappa)}, \tag{13}$$

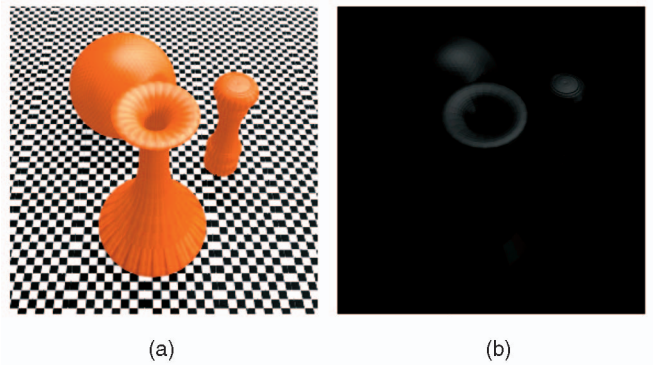

(a) (b)

Fig. 4. (a) Input image. (b) Specular reflection image.

$$q(l\,|\mathbf{x}_i,\Theta) \leftarrow \begin{cases} 1 & l = \underset{1\le h\le M_L}{\operatorname{argmax}}\ L_h f(\mathbf{x}_i|\boldsymbol{\mu}_h,\kappa) \\ 0 & \text{otherwise.} \end{cases} \tag{14}$$

2. **M Step**. Update each parameter for $l = 1,\ldots,M_L$ as

$$L_l \leftarrow \frac{1}{N}\sum_{i=1}^{N} p(l\,|\mathbf{x}_i,\Theta), \tag{15}$$

$$\boldsymbol{\mu}_l \leftarrow \frac{\sum_{i=1}^{N}\mathbf{x}_i\, p(l\,|\mathbf{x}_i,\Theta)}{\left\|\sum_{i=1}^{N}\mathbf{x}_i\, p(l\,|\mathbf{x}_i,\Theta)\right\|}, \tag{16}$$

$$\kappa \leftarrow \frac{N-1}{N-\sum_{i=1}^{N}\sum_{l=1}^{M_L} q(l\,|\mathbf{x}_i,\Theta)\mathbf{x}_i^T\boldsymbol{\mu}_l}. \tag{17}$$

Note that the number of component distributions is assumed to be known. Nevertheless, one of the advantages of solving this inverse rendering problem within the EM framework is that the optimal number of components, that is, the light source number (M_L) can be determined, as discussed in Section 3.3.

3.3 Light Source Number Estimation

The problem of determining the number of components in mixture models has been well studied in the statistical learning community [6], [33]. For instance, Cang and Partridge [3] used the Williams' statistical test to estimate the number of components in mixtures. Now, let us denote the parameters of the kth component distribution of the entire mixture distribution to be estimated with $\Theta_k^K = \{L_k^K, \boldsymbol{\mu}_k^K, \kappa^K\}$ $(k = 1,\ldots,K)$ when we assume that the number of mixture components is K. Then, the Kullback-Leibler divergence distance between the original vMF mixture density function, $\mathcal{P}(\mathbf{x})$ $(=\sum_{l=1}^{M_L} L_l f(\mathbf{x}\,|\boldsymbol{\mu}_l,\kappa) = \widetilde{I}_S(\mathbf{x}\,|\,\Theta))$, and the density function approximated by the estimated parameters Θ_k^K $(k = 1,\ldots,K)$, $\mathcal{P}^K(\mathbf{x}) = \sum_{k=1}^{K} L_k^K f(\mathbf{x}\,|\boldsymbol{\mu}_k^K,\kappa^K)$, becomes[2]

2. Strictly speaking, we should write $\mathcal{P}^K(\mathbf{x}\,|\Theta_1^K,\ldots,\Theta_K^K)$, but we drop $\Theta_1^K,\ldots,\Theta_K^K$ for simplicity.

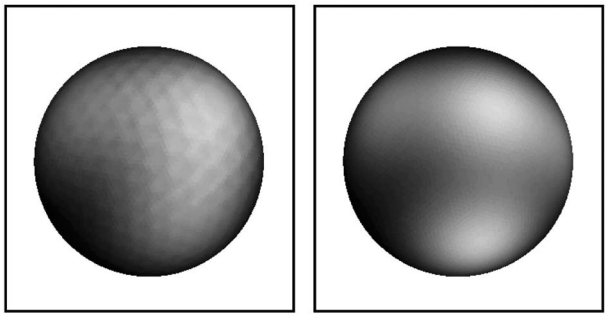

(a) (b)

Fig. 5. (a) Illumination sphere computed from Fig. 4b. (b) Illumination sphere estimated as a mixture of vMF distributions.

$$\begin{aligned} D(\mathcal{P},\mathcal{P}^K) &= \int_0^{2\pi}\!\!\int_0^{\pi} \mathcal{P}(\mathbf{x})\log\frac{\mathcal{P}(\mathbf{x})}{\mathcal{P}^K(\mathbf{x})}\sin\theta d\theta d\phi, \\ &= -\int_0^{2\pi}\!\!\int_0^{\pi} \mathcal{P}(\mathbf{x})\log\mathcal{P}^K(\mathbf{x})\sin\theta d\theta d\phi \\ &\quad + \int_0^{2\pi}\!\!\int_0^{\pi} \mathcal{P}(\mathbf{x})\log\mathcal{P}(\mathbf{x})\sin\theta d\theta d\phi. \end{aligned}$$

The first term Φ only depends on the number of components K and their corresponding mixture parameters Θ_k^K $(k = 1,\ldots,K)$ and can be approximated as

$$\Phi = E_p(-\log\mathcal{P}^K(\mathbf{x})) \approx -\frac{1}{N}\sum_{i=1}^{N}\log\mathcal{P}^K(\mathbf{x}_i), \tag{18}$$

where $E_p(\cdot)$ denotes the expectation value function, and $\{\mathbf{x}_1,\ldots,\mathbf{x}_N\}$ $(\|\mathbf{x}_i\| = 1, \forall i)$ is the data set consisting of N samples, as defined in the previous section. Clearly, as we increase the number of components, K, the estimated mixture density function becomes closer to the original density function. This means that the KL divergence $D(\mathcal{P},\mathcal{P}^K)$ will decrease as we increase K, which in turn means Φ decreases as K increases. Thus, intuitively, we can decide the optimal number of components K by evaluating the rate of change of Φ as we vary K.

Now, let $Y^K = -\log\mathcal{P}^K(\mathbf{x})$. Then, from (18), the mean, $\overline{Y}^K$, of Y^K represents the mean for different group level in Williams' test. For a given upper limit $\widetilde{K}$ of the candidate number of mixture components, the test statistic $\bar{t}_i$ in Williams' test is

$$\bar{t}_i = (\hat{M}_{\widetilde{K}+1-i} - \hat{M}_{\widetilde{K}})\Big(\frac{2s^2}{N}\Big)^{-1/2}, \quad (2 \le i \le \widetilde{K}), \tag{19}$$

where M_K $(1 \le K \le \widetilde{K})$ and s^2 are

$$\hat{M}_K = \ldots = \hat{M}_{K'} = \max_{K'\in[K,\widetilde{K}]}\sum_{l=K}^{K'}\frac{\overline{Y}^l}{K'-K+1}, \tag{20}$$

$$s^2 = \sum_{K=1}^{\widetilde{K}}\sum_{n=1}^{N}\frac{(Y_n^K - \overline{Y}^K)^2}{\nu}, \tag{21}$$

where Y_n^K is the nth individual in the Kth group and $\nu = \widetilde{K}(N-1)$ [3].

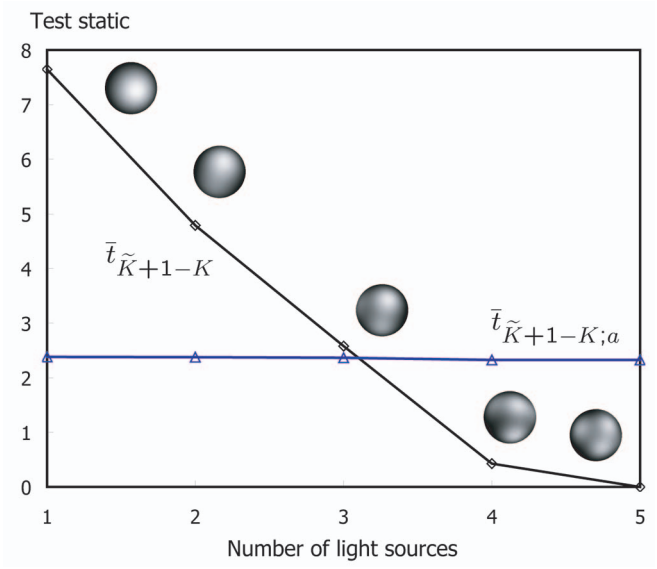

Fig. 6. Change in $\bar{t}_i$ as the number of mixture components decreases. Since $\bar{t}_2\ (K=4)$ is not significant, and $\bar{t}_3\ (K=3)$ is significant at $a=1$ percent level, we determine the number of mixture components (that is, light sources) as 4.

To solve the problem of estimating the number of light sources, we apply the algorithm in [3] in the following implementation.

1. Choose the upper limit $\widetilde{K}$ of the number of light sources. Set $i \leftarrow 1$. Set the light source number $K \leftarrow \widetilde{K}+1-i$.
2. Repeat Step 2a through Step 2c until $\bar{t}_i < \bar{t}_{i,a}$ ($\bar{t}_i$ is not significant at significance level a) and $\bar{t}_{i+1} > \bar{t}_{i+1,a}$ ($\bar{t}_{i+1}$ is significant at significance level a) are simultaneously satisfied, where $\bar{t}_{i,a}$ is the critical value at significance level a.
   a. Approximate the (normalized) illumination sphere with a mixture of K vMF probability density functions using the EM algorithm as described in Section 3.2, $\mathcal{P}^K(\mathbf{x})$.
   b. Calculate $\bar{t}_i$ in (9).
   c. $i \leftarrow (i+1)$, $K \leftarrow \widetilde{K}+1-i$.

Note that we assume that the scene illumination contains a number of discrete point light sources. Due to this assumption, we do not consider extended light sources such as fluorescent lamps in our method. However, if we can assume that the extended source consists of distant point sources with the same color and may manually enter the number of point sources, our method could be extended to model an extended source using a relatively small number of point sources.

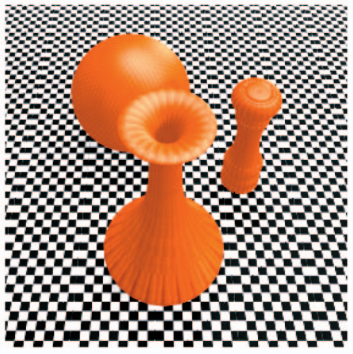

Fig. 7. Image synthesized using the estimated reflection parameter and illumination distribution.

3.4 Final Refinement

The estimates obtained in the last section may deviate a little from the true values, since the estimation algorithm is based on the spherical specular reflection model that approximates the Torrance-Sparrow reflection model. In this section, we improve those results through an optimization process based on the original Torrance-Sparrow reflection model. Note that we fix the number (M_L) and direction $(\boldsymbol{\mu}_l)$ of the light sources, since the algorithm described in the last sections is, as confirmed by our preliminary experiments, accurate with respect to these parameters.

Using the original (simplified) Torrance-Sparrow model, (9) can be modified as

$$\mathbf{I}_S \approx I_S \mathbf{L}, \tag{22}$$

$$I_S = \frac{1}{\cos\theta_r} \sum_{l=1}^{M_L} \widetilde{L}_l \exp\left[-\frac{\alpha_l^2}{2\sigma^2}\right], \tag{23}$$

where $\widetilde{L}_l = 2\pi K_S L_l / N_L$, $l = 1, \ldots, M_L$. This implies that estimation of K_S and L_l becomes an ill-posed problem. Therefore, we address the estimation of $\widetilde{L}_l$ in (23). The relative source radiance can be calculated by normalizing each $\widetilde{L}_l$ so that $\sum_{l=1}^{M_L} \widetilde{L}_l = 1$.

Now, we reestimate $\widetilde{L}_l$ and σ by solving the optimization problem as

$$\underset{\widetilde{\Theta}}{\operatorname{argmin}} \sum_{(s,t)=(0,0)}^{N_S,N_T} |I(s,t) - I_S(s,t)|^2, \tag{24}$$

where $\widetilde{\Theta} = \{\widetilde{L_1}, \ldots, \widetilde{L_{M_L}}, \sigma\}$, $I(s,t)$ is the image irradiance of the observed (separated) specular reflection component, and (N_S, N_T) is the numbers of horizontal and vertical

TABLE 1
Estimation Results

	Light 1	Light 2	Light 3	Light 4
Estimated light direction	$(0.490, 0.075, -0.868)$	$(0.551, 0.833, -0.045)$	$(0.880, 0.168, 0.445)$	$(0.0373, 0.942, -0.333)$
Ground truth	$(0.497, 0.109, -0.861)$	$(0.531, 0.822, -0.204)$	$(0.861, 0.274, 0.429)$	$(0.0208, 0.943, -0.333)$
Estimated light intensity	0.204	0.294	0.141	0.361
Ground truth	0.2	0.3	0.15	0.35

pixels, respectively. To solve (24), we utilize an iterative approach, as described in the following procedures.

First, we set the initial values of $\widetilde{L}_l$ and σ as

$$\widetilde{L_l^0} = \gamma^* L_l^*, \tag{25}$$

$$\sigma^0 = \frac{1}{2\sqrt{\kappa^*}}, \tag{26}$$

where L_l^* and κ^* are the (initial) estimates of L_l and κ obtained in the last section, respectively, and γ^* is the solution to the following linear least squares problem:

$$\gamma^* = \underset{\gamma}{\operatorname{argmin}} \sum_{(s,t)=(0,0)}^{N_S,N_T} |I(s,t) - \gamma\, I_S^*(s,t)|^2, \tag{27}$$

where I_S^* represents the specular image synthesized using the estimates that we obtained in the last sections. Next, we alternate between gradient descent minimization of (24) with respect to $\widetilde{L}_l$ and σ until convergence [21].

We now assume that the diffuse reflectance property of the surface can be approximated with a Lambertian reflection model. In this case, we are able to synthesize the new diffuse image by computing the ratio of irradiance between the original and new lighting condition for each surface point. Then, by synthesizing the new specular image with the estimated illumination and specular parameters, and adding those diffuse and specular images, we are able to render the virtual object image under the new lighting condition [21].

4 Experimental Results

To demonstrate and evaluate our method, we chose to use a synthetic image and two real images as inputs. In all the experiments, we used a geodesic dome consisting of approximately 4,100 vertices. We searched for the optimal number of light sources in the interval from 1 to 5 ($\widetilde{K} = 5$). We randomly drew 1,000 samples ($\mathcal{X}$) from the normalized illumination sphere (that is, a mixture of vMF distributions), as described in Section 3.2.

4.1 Synthetic Image

In this experiment, we rendered an input image of a scene consisting of multiple objects with a relatively large roughness value using RADIANCE [24]. Fig. 4a shows the input image. From the specular reflection image (Fig. 4b), we computed the illumination sphere (Fig. 5a), as discussed in Section 3.1. Then, we normalized the illumination sphere ((12)) and approximated it with a finite mixture of vMF distributions while varying the number of components, as explained in Sections 3.2 and 3.3. Fig. 6 shows the effects of decreasing the number of mixture components. The vertical axis represents the value of the Student's t-distribution. The horizontal axis represents the setting number (K) of mixture components. In Fig. 6, at the correct number of components $K = 4$ ($i = \widetilde{K} + 1 - K = 2$), the two criteria $\overline{t}_i < \overline{t}_{i,a}$ and $\overline{t}_{i+1} > \overline{t}_{i+1,a}$ are simultaneously satisfied and, thus, the number of light sources can be determined as 4. Fig. 5b shows the illumination sphere approximated with a mixture of vMF distributions for the estimated number of components. The synthetic image in Fig. 7 was generated using the estimated parameters. The directions and intensities of light sources are tabulated in Table 1. The estimate of the roughness parameter σ is 0.185. Since RADIANCE uses the Ward reflection model [36], the estimated roughness parameter cannot be directly compared to the ground-truth value. Nevertheless, the light sources including their directions and intensities are recovered accurately, which in turn indicates that the roughness parameter is also estimated accurately. Fig. 8 shows ground truth images and synthetic images rendered under novel lighting conditions in which only one light source of the four is turned on in each pair. We can see that the target objects and their shadows cast on the table are

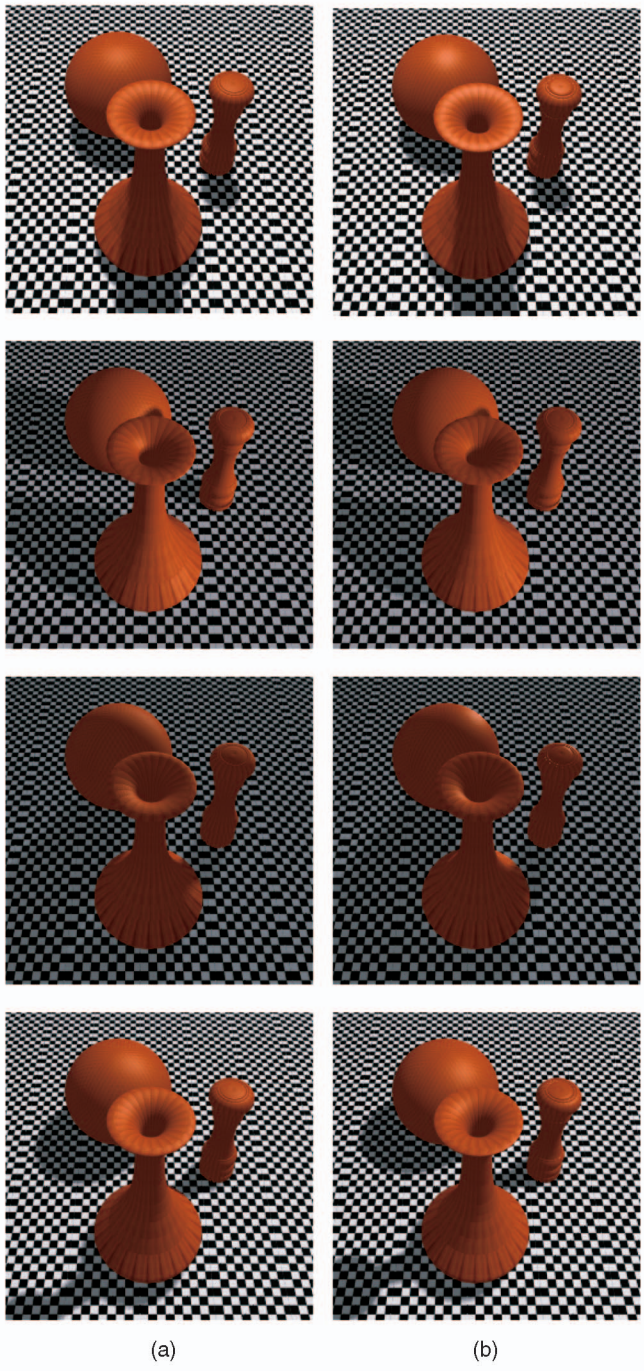

Fig. 8. Images under each point light source. (a) Original images and (b) synthesized images.

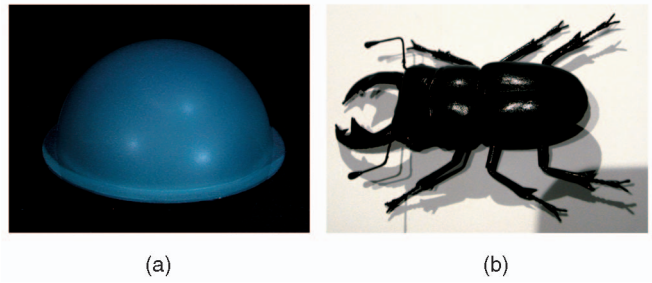

Fig. 9. Input images. (a) Hemispherical object. (b) Beetle object.

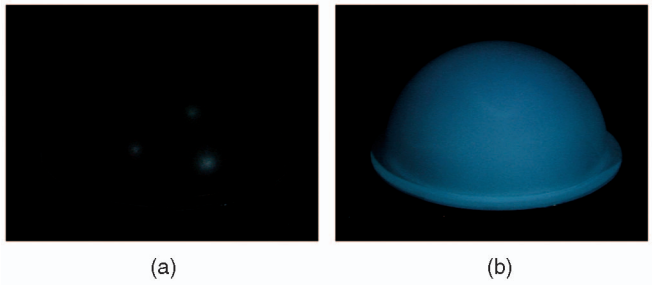

Fig. 10. Reflection components separated from Fig. 9a. (a) Specular reflection image. (b) Diffuse reflection image.

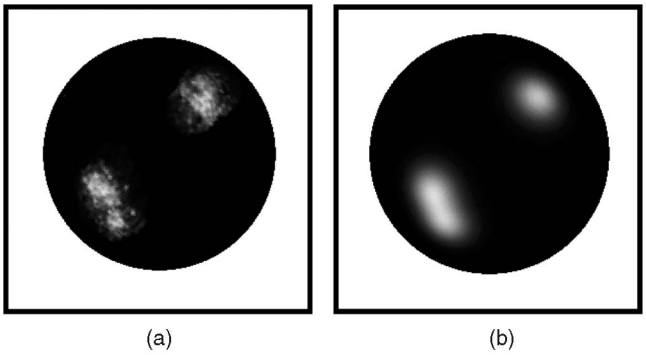

Fig. 11. (a) Illumination sphere computed from that in Fig. 9b. (b) Illumination sphere estimated as a mixture of vMF distributions.

rendered correctly. As a result, even with such a relatively large roughness, we are able to estimate how each light source separately contributes to the original scene appearance.

4.2 Real Image

We also conducted experiments on real objects. The objects we use in our experiments are a hemispherical object made of Fiber Reinforced Plastic (FRP) and a replica of a beetle made of Polyvinyl Chloride (PVC). Fig. 9 shows an input image for each object. Note that the specular highlights in Fig. 9b partially overlap. For each object, color images are captured using a color CCD video camera. We obtain a 3D geometric model for each object using a light-stripe range finder with a liquid crystal shutter and a contact digitizer, respectively. For the hemispherical object, we use a polarization filter [9] to separate the diffuse and specular reflection components, as shown in Fig. 10. Note that other techniques, including color-based methods [30], can be used instead and that the beetle object does not have the diffuse reflection component but only the specular reflection component.

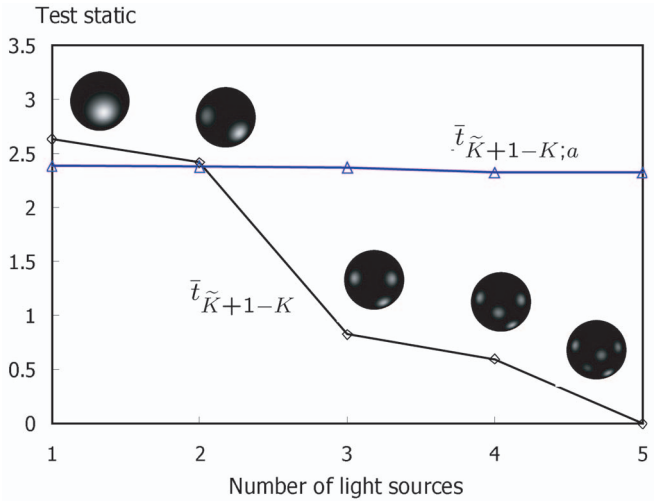

Fig. 12. Change in $\bar{t}_i$ as the number of mixture components decreases (the hemispherical object). Since $\bar{t}_3\ (K=3)$ is not significant, and $\bar{t}_4\ (K=2)$ is significant at $a=1$ percent level, we determine the number of mixture components (that is, light sources) as 3.

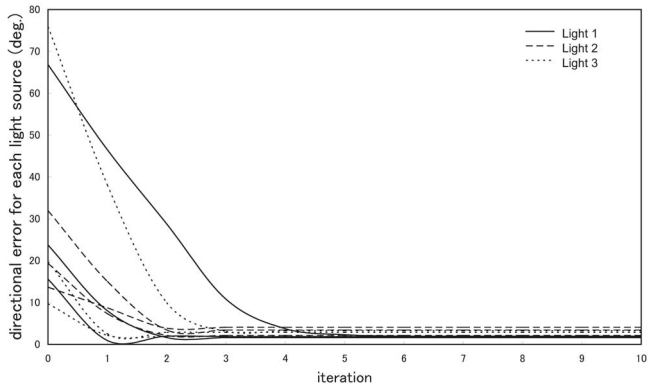

Fig. 13. Learning curves of our EM algorithm for the estimation of the light sources. The curves show the directional error for the three point light sources consisting the illumination environment. The solid line, the dashed line, and the dotted line correspond to the first source (Light 1), the second source (Light 2), and the third source (Light 3), respectively. Different curves for the same light source depict results from different initial estimates. The estimates converge fairly quickly with a couple of iterations regardless of the initial error.

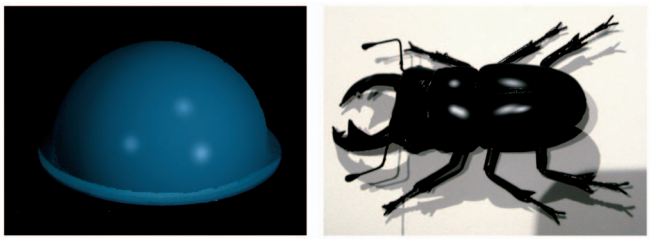

Fig. 14. Synthetic images rendered using the estimated reflection parameter and illumination distribution.

We obtained Figs. 11 and 12 and correctly estimated the number of light sources as 3 in the same way as in the cases in Figs. 5 and 6. Fig. 13 shows the results of testing the robustness to initial values and convergence of our EM algorithm. These results show that the EM algorithm in our method converges fast, independent of the initial state. As shown in Fig. 14, we rendered these input scenes using the estimated reflection parameters and lighting conditions. The directions and

TABLE 2
Estimation Results for the Hemispherical Object

	Light 1	Light 2	Light 3
Estimated light direction	$(-0.873, -0.134, 0.470)$	$(-0.012, -0.962, 0.272)$	$(0.084, -0.442, 0.893)$
Ground truth	$(-0.898, -0.119, 0.423)$	$(-0.0469, -0.978, 0.2)$	$(0.0379, -0.517, 0.855)$
Estimated light intensity	0.291	0.432	0.276
Ground truth	0.276	0.444	0.280

TABLE 3
Estimation Results for the Beetle Object

	Light 1	Light 2	Light 3
Estimated light direction	$(-0.223, -0.106, 0.969)$	$(0.813, 0.039, 0.580)$	$(-0.106, 0.109, 0.988)$
Ground truth	$(-0.220, -0.139, 0.966)$	$(0.772, -0.025, 0.635)$	$(-0.204, 0.048, 0.978)$
Estimated light intensity	0.345	0.314	0.341
Ground truth	0.350	0.308	0.342

intensities of light sources are tabulated in Tables 2 and 3. The estimates of σ were 0.0749 and 0.0576 for the hemispherical and beetle objects, respectively. Figs. 15 and 16 show the results of synthesizing the object's appearance under novel lighting conditions in the same way as Fig. 8 except that the shadows are not rendered. One can see that these images relit by our method are nearly exact for real images.

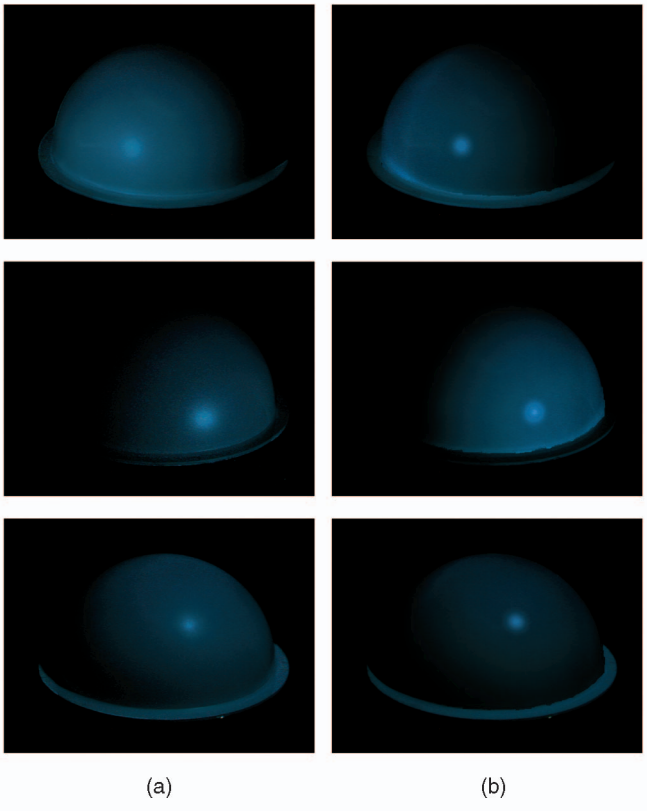

Fig. 15. Images under each point light source for the hemisphere object. (a) Original photographs and (b) synthesized images.

5 Conclusions

Given single-view images taken under multiple point light sources and a geometric model of the target object in the scene, we have proposed a method to simultaneously estimate the illumination condition and the surface reflectance property based on a rigorous directional statistics approach. By first representing the specular reflection as a mixture of probability distributions on the unit sphere and then using the EM algorithm to estimate the mixture

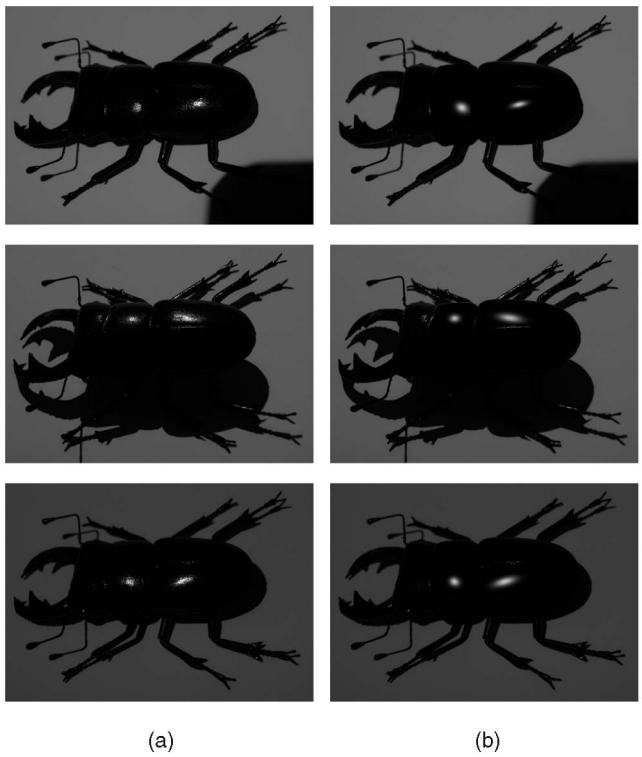

Fig. 16. Images under each point light source for the beetle object. (a) Original photograph and (b) synthesized images.

parameters, we are able to estimate not only the direction and intensity of the light sources but also the number of light sources and the specular reflectance property. We can use the results to render the object under novel lighting conditions. These results clearly demonstrate the advantage of using a directional statistics based approach for inverse rendering. We believe that other reflectance models described with half-angle vector parameterization can be incorporated albeit minor modifications in the derivation. We also believe that multiple images [18], [40], [39], [20], [21], [43], [28] will increase the sampling density of the mixture of vMF distributions and, hence, increase the accuracy of the estimates. The future works include recovery of nonhomogeneous specular reflectance properties and the distances to light sources.

ACKNOWLEDGMENTS

The work described in this paper was, in part, supported by Japan Science and Technology (JST) under CREST Ikeuchi Project, and by the Japanese Ministry of Education, Science, and Culture under the Grant in Aid for Scientific Research 17500113.

REFERENCES

[1] A. Banerjee, I. Dhillon, J. Ghosh, and S. Sra, "Generative Model-Based Clustering of Directional Data," *Proc. Ninth ACM SIGKDD Int'l Conf. Knowledge Discovery and Data Mining,* pp. 19-28, 2003.

[2] S. Boivin and A. Gagalowicz, "Image-Based Rendering of Diffuse, Specular and Glossy Surfaces from a Single Image," *Proc. ACM SIGGRAPH,* pp. 197-216, 2001.

[3] S. Cang and D. Partridge, "Determining the Number of Components in Mixture Models using Williams' Statistical Test," *Proc. Eighth Int'l Conf. Neural Information Processing,* pp. 14-18, 2003.

[4] A.P. Dempster, N.M. Laird, and D.B. Rubin, "Maximum-Likelihood from Incomplete Data via the EM Algorithm," *J. Royal Statistical Soc. B,* pp. 1-38, 1977.

[5] G. Drettakis, L. Robert, and S. Bougnoux, "Interactive Common Illumination for Computer Augmented Reality," *Proc. Eurographics Rendering Workshop,* pp. 45-56, 1997.

[6] M. Figueiredo and A.K. Jain, "Unsupervised Learning of Finite Mixture Models," *IEEE Trans. Pattern Analysis and Machine Intelligence,* vol. 24, no. 3, pp. 381-396, Mar. 2002.

[7] R.A. Fisher, "Dispersion on a Sphere," *Proc. Royal Soc. London, Series A,* vol. 217, pp. 295-305, 1953.

[8] A. Fournier, A.S. Gunawan, and C. Romanzin, "Common Illumination between Real and Computer Generated Scenes," *Proc. Graphics Interface,* pp. 254-262, 1993.

[9] K. Hara, K. Nishino, and K. Ikeuchi, "Determining Reflectance and Light Position from a Single Image without Distant Illumination Assumption," *Proc. lnt'l Conf. Computer Vision,* pp. 560-567, 2003.

[10] D.R. Hougen and N. Ahuja, "Estimation of the Light Source Distribution and Its Use in Integrated Shape Recovery from Stereo Shading," *Proc. Int'l Conf. Computer Vision,* pp. 148-155, 1993.

[11] K. Ikeuchi and K. Sato, "Determining Reflectance Properties of an Object Using Range and Brightness Images," *IEEE Trans. Pattern Analysis and Machine Intelligence,* vol. 13, no. 11, pp. 1139-1153, Nov. 1991.

[12] C.-Y. Kim, A.P. Petrov, H.-K. Choh, Y.-S. Seo, and I.-S. Kweon, "Illuminant Direction and Shape of a Bump," *J. Optical Soc. Am. A,* vol. 15, no. 9, pp. 2341-2350, 1998.

[13] G. Klinker, S. Shafer, and T. Kanade, "A Physical Approach to Color Image Understanding," *lnt'l J. Computer Vision,* vol. 4, pp. 7-38, 1990.

[14] Y. Li, S. Lin, H. Lu, and H. Shum, "Multiple-Cue Illumination Estimation in Textured Scenes," *Proc. Int'l Conf. Computer Vision,* pp. 1366-1373, 2003.

[15] K.V. Mardia and P.E. Jupp, *Directional Statistics.* John Wiley & Sons, 2000.

[16] S.R. Marschner and D.P. Greenberg, "Inverse Lighting for Photography," *Proc. Fifth Color Imaging Conf., Soc. Imaging Science and Technology,* pp. 262-265, 1997.

[17] D. Miyazaki, R.T. Tan, K. Hara, and K. Ikeuchi, "Polarization-Based Inverse Rendering from a Single View," *Proc. Int'l Conf. Computer Vision,* pp. 982-987, 2003.

[18] N. Mukawa, "Estimation of Shape, Reflection Coefficients and Illuminant Direction from Image Sequences," *Proc. Int'l Conf. Computer Vision,* pp. 507-512, 1990.

[19] S. Nayar, K. Ikeuchi, and T. Kanade, "Surface Reflection: Physical and Geometrical Perspectives," *IEEE Trans. Pattern Analysis and Machine Intelligence,* vol. 13, no. 7, pp. 611-634, July 1991.

[20] K. Nishino, Z. Zhang, and K. Ikeuchi, "Determining Reflectance Parameters and Illumination Distribution from a Sparse Set of Images for View-Dependent Image Synthesis," *Proc. Int'l Conf. Computer Vision,* pp. 599-606, 2001.

[21] K. Nishino, K. Ikeuchi, and Z. Zhang, "Re-Rendering from a Sparse Set of Images," Technical Report DU-CS-05-12, Dept. of Computer Science, Drexel Univ., Nov. 2005.

[22] T. Okabe, I. Sato, and Y. Sato, "Spherical Harmonics vs. Haar Wavelets: Basis for Recovering Illumination from Cast Shadows," *Proc. Conf. Computer Vision and Pattern Recognition,* pp. 50-57, 2004.

[23] A.P. Pentland, "Finding the Illumination Direction," *J. Optical Soc. Am. A,* vol. 72, no. 4, pp. 448-455, 1982.

[24] http://radsite.lbl.gov/radiance/HOME.html, 1997.

[25] R. Ramamoorthi and P. Hanrahan, "A Signal-Processing Framework for Inverse Rendering," *Proc. ACM SIGGRAPH,* pp. 117-128, 2001.

[26] I. Sato, Y. Sato, and K. Ikeuchi, "Illumination from Shadows," *IEEE Trans. Pattern Analysis and Machine Intelligence,* vol. 25, no. 3, pp. 290-300, Mar. 2003.

[27] S. Shafer, "Using Color to Separate Reflection Components," *COLOR Research and Application,* vol. 10, no. 4, pp. 210-218, 1985.

[28] L. Shen and H. Takemura, "Spatial Reflectance Recovery Under Complex Illumination from Sparse Images," *Proc. Conf. Computer Vision and Pattern Recognition,* pp. 1833-1838, 2006.

[29] F. Solomon and K. Ikeuchi, "Extracting the Shape and Roughness of Specular Lobe Objects Using Four Light Photometric Stereo," *Proc. Conf. Computer Vision and Pattern Recognition,* pp. 466-471, 1992.

[30] R.T. Tan and K. Ikeuchi, "Separating Reflection Components of Textured Surfaces from a Single Image," *IEEE Trans. Pattern Analysis and Machine Intelligence,* vol. 27, no. 2, pp. 178-193, Feb. 2005.

[31] S. Tominaga and N. Tanaka, "Estimating Reflection Parameters from a Single Color Image," *IEEE Computer Graphics and Applications,* vol. 20, no. 5, pp. 58-66, Sept./Oct. 2000.

[32] K.E. Torrance and E.M. Sparrow, "Theory of Off-Specular Reflection from Roughened Surfaces," *J. Optical Soc. Am. A,* vol. 57, pp. 1105-1114, 1967.

[33] J. Verbeek, N. Vlassis, and B. Krose, "Efficient Greedy Learning of Gaussian Mixture Models," *Neural Computation,* vol. 15, no. 2, pp. 469-485, 2003.

[34] Y. Wang and D. Samaras, "Estimation of Multiple Illuminants from a Single Image of Arbitrary Known Geometry," *Proc. European Conf. Computer Vision,* pp. 272-288, 2002.

[35] Y. Wang and D. Samaras, "Estimation of Multiple Directional Light Sources for Synthesis of Augmented Reality Images," *Graphical Models,* vol. 65, no. 4, pp. 185-205, 2003.

[36] G. Ward, "Measuring and Modeling Anisotoropic Reflection," *Proc. ACM SIGGRAPH '92,* pp. 265-272, 1992.

[37] G.S. Watson and E.J. Williams, "On the Construction of Significance Tests on the Circle and the Sphere," *Biometrika,* vol. 43, pp. 344-352, 1956.

[38] Y. Yang and A. Yuille, "Source from Shading," *Proc. Conf. Computer Vision and Pattern Recognition,* pp. 534-539, 1991.

[39] Y. Yu, P. Debevec, J. Malik, and T. Hawkins, "Inverse Global Illumination: Recovering Reflectance Models of Real Scenes from Photographs," *Proc. ACM SIGGRAPH,* pp. 215-224, 1999.

[40] Y. Yu and J. Malik, "Recovering Photometric Properties of Architectural Scenes from Photographs," *Proc. ACM SIGGRAPH,* pp. 207-217, 1998.

[41] Y. Zhang and Y.H. Yang, "Multiple Illuminant Direction Detection with Application to Image Synthesis," *IEEE Trans. Pattern Analysis and Machine Intelligence,* vol. 23, no. 8, pp. 915-920, Aug. 2001.

[42] Q. Zheng and R. Chellappa, "Estimation of Illuminant Direction, Albedo, and Shape from Shading," *IEEE Trans. Pattern Analysis and Machine Intelligence,* vol. 13, no. 7, pp. 680-702, July 1991.
[43] W. Zhou and C. Kambhamettu, "Estimation of Illuminant Direction and Intensity of Multiple Light Sources," *Proc. European Conf. Computer Vision,* pp. 206-220, 2002.

Kenji Hara received the BE and ME degrees from Kyoto University in 1987 and 1989, respectively, and the PhD degree from Kyushu University in 1999. He then held several positions at Takeda Pharmaceutical Co. Ltd. and Fukuoka Industrial Technology Center, Japan. Since 2001, he has been an adjunctive researcher at the University of Tokyo. In 2004, he joined Kyushu University, where he is currently an associate professor at the Department of Visual Communication Design. His research interests include physics-based vision and geometric modeling. He is a member of the IEEE.

Ko Nishino received the BE and ME degrees in information and communication engineering and the PhD degree in information science from the University of Tokyo in 1997, 1999, and 2002, respectively. He is an assistant professor at the Department of Computer Science, Drexel University. Prior to joining Drexel University in 2005, he worked as a postdoctoral research scientist at the Department of Computer Science, Columbia University. His research interests span computer vision and computer graphics. The main focus of his research is on photometric and geometric modeling of real-world objects and scenes. He has published a number of papers on related topics, including physics-based vision, image-based modeling and rendering, and recognition. He is a member of the IEEE and the ACM.

Katsushi Ikeuchi received the BE degree from Kyoto University in 1973 and the PhD degree from the University of Tokyo in 1978. After working at the Massachusetts Institute of Technology (MIT) Artificial Intelligence (AI) Laboratory for three years, ETL for five years, and Carnegie Mellon University (CMU) Robotics Institute for 10 years, he joined the University of Tokyo in 1996 and is currently a full professor. His research interest spans computer vision, robotics, and computer graphics. In these research fields, he has received several awards, including the David Marr Prize in computational vision for the paper "Shape from Interreflection," and IEEE Robotics and Automation Society K.S. Fu memorial best transaction paper award for the paper "Toward Automatic Robot Instruction from Perception—Mapping Human Grasps to Manipulator Grasps." In addition, in 1992, his paper "Numerical Shape from Shading and Occluding Boundaries" was selected as one of the most influential papers to have appeared in the *Artificial Intelligence Journal* within the past 10 years. His IEEE activities include general chair of IROS '95, ITSC '00, IV '01; program chair of the CVPR '96 and ICCV '03; associate editor of *IEEE Transactions on Robotics and Automation*, *IEEE Transactions on Pattern Analysis and Machine Intelligence*; and a distinguished lecturer of the Signal Processing Society in 2000-2002 and Robotics and Automation Society in 2004-2006. He was elected an IEEE fellow in 1998. He is the editor-in-chief of the *International Journal of Computer Vision*.